DMD Fast Forward. Published on January 12, 2007 as doi:10.1124/dmd.106.012336
This article has not been copyedited and formatted. The final version may differ from this version.

METABOLISM AND EXCRETION OF RWJ-333369 IN MICE, RATS, RABBITS, AND DOGS

Rao N.V.S Mamidi, Geert Mannens, Pieter Annaert, Jan Hendrickx, Ivo Goris, Mark Bockx, Cor G. M. Janssen, Mark Kao, Michael F. Kelley, and Willem Meuldermans

Department of Preclinical Drug Development, Johnson & Johnson Pharmaceutical Research & Development, Raritan, NJ, USA [R.N.V.S.M., M.K]; Department of Preclinical Drug Development, Johnson & Johnson Pharmaceutical Research & Development, Spring House, PA, USA [M.F.K.]; and Department of Preclinical Pharmacokinetics, Johnson & Johnson Pharmaceutical Research & Development, a division of Janssen Pharmaceutica N.V., Beerse, Belgium [G.M., P.A., J.H., I.G., M.B., C.G.M.J., W.M.]

Running title

RWJ-333369 metabolism and excretion in preclinical species

Address correspondence to:

Rao N.V.S. Mamidi, PhD

Preclinical Drug Development, OMP-2211

Johnson & Johnson Pharmaceutical Research & Development

1000 US 202 S

Raritan, NJ 08807, USA

Phone: (908) 704 4262

Fax: (908) 253 0448

Email: smamidi1@prdus.jnj.com

Number of text pages: 23

Number of tables: 6

Number of figures: 8

Number of references: 13

Word count:

Abstract: (250 max): 239

Introduction (750 max): 189

Discussion (1500 max): 1099

Nonstandard abbreviations

APCI = atomospheric pressure chemical ionization; CPG = 2-chlorophenylglycine; CBA = 2-chlorobenzoic acid; CMA = 2-chloromandelic acid; dpm = disintegrations per minute; ESI = electrospray ionization; GAERS = genetic absence epilepsy rat from Strasbourg; HPLC = high performance liquid chromatography; LC-MS/MS = liquid chromatography-tandem mass spectrometry; MAC = mercapturic acid; NAC = N-acetyl-cysteine; PDA = photodiode-array detector; pre-MACs = premercapturic acid conjugates; QTof = hybrid quadrupole time-of-flight mass spectrometry; RI = regioisomer; TMS = tetramethylsilane; TR = total radioactivity; and UD = unchanged drug.

DMD Fast Forward. Published on January 12, 2007 as DOI: 10.1124/dmd.106.012336
This article has not been copyedited and formatted. The final version may differ from this version.

Abstract

The *in vivo* metabolism and excretion of RWJ-333369 [1,2-ethanediol, 1-(2-chlorophenyl)-, 2-carbamate, (S)], a novel neuromodulator, were investigated in mice, rats, rabbits, and dogs after oral administration of ^{14}C-RWJ-333369. Plasma, urine, and feces samples were collected, assayed for radioactivity, and profiled for metabolites. In almost all species, the administered radioactive dose was predominantly excreted in urine (>85%) with less than 10% in feces. Excretion of radioactivity was rapid and nearly complete at 96 h after dosing in all species. Unchanged drug excreted in urine was minimal (<2.3% of the administered dose) in all species. The primary metabolic pathways were *O*-glucuronidation (rabbit > mouse > dog > rat) of RWJ-333369 and hydrolysis of the carbamate ester followed by oxidation to 2-chloromandelic acid. The latter metabolite was subsequently metabolized in parallel to 2-chlorophenylglycine and 2-chlorobenzoic acid (combined hydrolytic and oxidative pathways: rat > dog > mouse > rabbit). Other metabolic pathways present in all species included chiral inversion in combination with *O*-glucuronidation and sulphate conjugation (either directly and/or following hydroxylation of RWJ-333369). Species-specific pathways, including N-acetylation of 2-chlorophenylglycine (mice, rats, and dogs) and arene oxidation followed by glutathione conjugation of RWJ-333369 (mice and rats), were more predominant in rodents than in other species. Consistent with human metabolism, multiple metabolic pathways and renal excretion were mainly involved in the elimination of RWJ-333369 and its metabolites in animal species. Unchanged drug was the major plasma circulating drug-related substance in the preclinical species and humans.

Introduction

RWJ-333369 (1,2-ethanediol, 1-(2-chlorophenyl)-, 2-carbamate, (S)- and CAS Registry Number 194085-75-1) is a new neuromodulator currently under clinical investigation for adjunctive treatment of epilepsy. In preclinical studies (data on file), this drug has demonstrated broad anticonvulsant activity, both elevating seizure threshold and preventing seizure spread. It has shown efficacy in attenuating the frequency and severity of spontaneous recurrent seizures in kainite-treated rats (Grabenstatter and Dudek, 2004) and suppressing spike-and-wave discharges in the GAERS (Genetic Absence Epilepsy Rat from Strasbourg) model of idiopathic generalized epilepsy (Nehlig et al., 2005).

The objective of the present study was to determine the absorption, metabolism, and excretion of RWJ-333369 in preclinical species (mice, rats, rabbits and dogs) and to identify and quantify its major and minor metabolites following a single oral dose of ^{14}C-radiolabeled RWJ-333369. The urinary and fecal excretion (mass balance) and the blood and plasma radioactivity levels were determined by liquid scintillation counting. Metabolite profiling and identification of these metabolites were done by high performance liquid chromatography (HPLC) with radioactivity detection and liquid chromatography-tandem mass spectrometry (LC-MS/MS) analysis. Information generated from this study was used to support the nonclinical safety evaluation of RWJ-333369.

Materials and methods

Test article

RWJ-333369, specifically labeled with ^{14}C at the benzylic carbon (Fig. 1.) was synthesized by Johnson & Johnson Pharmaceutical Research & Development (Belgium). The ^{14}C-label at this position has been proven to be metabolically stable, as evidenced from the lack of $^{14}CO_2$ exhalation in the rat after oral dosing of ^{14}C-RWJ-333369. The radiolabeled substance had a specific activity of 998 MBq/mmol (or 4.6 MBq/mg) and a radiochemical purity of 98.9%. The enantiomeric excess determined by chiral-radio-HPLC method was found to be 98.7%. Unlabelled RWJ-333369 was synthesized by Janssen-Cilag (Switzerland) and had a chemical purity of 100%. Appropriate amounts of radiolabeled and unlabeled RWJ-333369 were combined to adjust the specific activity for dosing. For the identification of metabolites various synthetic reference compounds were used and the synthetic procedure were not detailed in this article (data on file).

Animal experiments

All animal experiments were conducted according to protocols approved by the Johnson & Johnson animal care and use committee. All animals were treated with a single dose of ^{14}C-RWJ-333369 followed by collection of plasma, urine and feces at pre-defined intervals (see individual studies below). At the end of sample collections, cage debris and cage washings were collected for determination of total radioactivity (TR) mass balance.

Mouse study. Twenty-four male and twenty-four female SPF Albino (CD1) mice (approximately 6-8 weeks of age) were obtained from Charles River (Kent, UK). Animals were divided into groups A and B within each sex, the former group was used for generating plasma metabolite

profiles and the latter for the metabolism-excretion balance study. Group A animals were placed and acclimatized in grid-bottomed polypropylene cages (4 per cage of same sex) and group B were placed in glass metabolism cages (4 per cage of same sex). A suspension of ^{14}C-RWJ-333369 in 0.5% Methocel F4M Premium EP was prepared with a specific activity of 70 kBq/mg and the mice were dosed orally by gavage at 50 mg/kg dose (3.5 MBq/kg). The dose of 50 mg/kg corresponded to the low dose in an oral mouse carcinogenicity study with RWJ-333369. Plasma samples were collected from group A animals at 1 h, 3 h, 8 h and 24 h post dose intervals (3 mice per time point per sex) and urine and feces were collected from group B animals from 0 to 96 h post dose at defined time intervals (0-12 h, 24-48 h, 48-72 h and 72-96 h for urine and every 24 h for 4 days of feces).

Rat study. Twenty male and twenty female young Sprague-Dawley rats (approximately 8-9 weeks of age) were obtained from Charles River (Sulzfeld, Germany). Animals were divided into two groups A and B within each sex, the former group was used for generating plasma metabolite profiles and the latter for the metabolism-excretion balance study. Per sex, animals from the pharmacokinetics group were placed and acclimatized in macrolon cages (3 per cage, total 12 animals) and animals for mass balance and metabolic profiling were placed in stainless steel metabolic cages (1 per cage, total 5 animals per sex). Remaining animals were kept as reserve animals. A solution (in water) of ^{14}C-RWJ-333369 was prepared with a specific activity of 49.3 kBq/mg, and the rats were dosed orally by gavage at 30 mg/kg dose (0.36 MBq for males and 0.31 MBq for females). The dose of 30 mg/kg corresponded to the low dose in a 3-month oral rat toxicity study. Plasma samples were collected from group A animals at 1 h, 3 h, 8 h and 24 h post dose intervals (3 per time point per sex) and urine and feces were collected from metabolism group (group B) animals from 0 to 96 h post dose at defined time intervals.

Rabbit study. After acclimatization period, two of the four female New Zealand white albino rabbits (approximately 16-30 weeks of age, procured from Centre Lago , France) were dosed orally by gavage at 100 mg/kg dose (~5.54 MBq) and the third rabbit received 200 mg/kg dose (~10.52 MBq) with a suspension of ^{14}C-RWJ-333369 in 0.5% Methocel (F4M Premium EP) (specific activity of 16.7 kBq/mg). The one remaining rabbit was kept as a reserve animal. The dose of 200 mg/kg corresponded to the highest dose used in an oral developmental toxicity study in the rabbit. Plasma samples were collected at 1 h, 2 h, 3 h, 4 h, 8 h, 24 h, 48 h and 72 h after dosing. Urine was collected from 0-24 h, 24-48 h and 48-72 h after dose administration. Feces were collected daily for up to 3 days (72 h) after dosing and weights were recorded.

Dog study. After acclimatization period, four of the six dogs (Janssen Animal Breeding Centre, Belgium) were dosed orally by gavage at 20 mg/kg dose (~12.39 MBq) with a solution of ^{14}C-RWJ-333369 (specific activity: 49.3 kBq/mg). The two remaining dogs were kept as reserve animals. The oral dose of 20 mg/kg corresponded to the low dose level in a 3-month oral toxicity study in the dog. Plasma samples were collected at 0.25 h, 0.5 h, 1 h, 1.5 h, 2 h, 4 h, 6 h, 8 h, 24 h, 32 h, 48 h, 72 h, 96 h, and 168 h after dosing. Urine was collected once before dosing and in intervals of 0-4 h, 4-8 h, 8-24 h, 24-48 h, 72-96 h, 120-144 h and 144-168 h after dose administration. Feces were collected daily for 7 days after dosing and weights were recorded.

Sample analysis

Predose plasma, urine, and feces samples of all test species were spiked with known quantities of ^{14}C-RWJ-333369 and stored during the period of the studies to allow verification of the stability of the drug in these media.

Mass balance-radioactivity. The TR was measured in all urine and plasma samples that were collected at various intervals in all studies. Aliquots of urine (0.25 mL in case of rats, rabbits,

and dogs and 0.20 mL in case of mice) in duplicates were mixed with 10 mL of Ultima Gold (Packard) as scintillation cocktail. The TR in urine samples was determined by liquid scintillation counting using a Packard Tri-Carb 2100 TR liquid scintillation spectrometer (Meriden, CT). Similarly, the TR in plasma samples of animal species was measured in duplicate aliquots.

For the measurement of TR in the feces samples, each sample was extracted with 3 different aliquots of methanol using a homogenizer (Ultra-Turrax, Janke and Kunkel GmbH and Co., Germany) and a Büchner funnel (Merck Eurolab Holding GmbH, Belgium). The radioactivity was measured in duplicate aliquots of the resultant pooled methanolic extracts by liquid scintillation spectrometer after mixing with water and 10 mL Ultima Gold scintillation cocktail (Packard). The fecal residues after methanolic extraction were air-dried and ground to a fine powder in an ultra centrifugal mill. Four weighed aliquots of each homogenized sample of about 80-120 mg were weighed in Combusto-cones (Packard) and combusted in a Packard Sample Oxidiser model 307. Carbosorb (8 mL; Packard) was used to absorb the $^{14}CO_2$ and Permafluor (Packard) was used as scintillation cocktail. The radioactivity in the combusted fecal residues was measured by liquid scintillation counting, using Packard Tri-Carb 1900TR or 2100TR scintillation spectrometer. The TR in feces was calculated as the sum of the radioactivity in the methanolic fecal extracts and the feces residues.

Sample preparation for metabolite profiling. Where appropriate, per gender, per time interval (eg: 0-12 h, 12-24 h, 24-48 h, etc), urine pools or methanolic extract pools were prepared by mixing constant fractions of the original sample volume collected during the same interval across the subjects. The overall urine or methanolic extract pools across a broader time interval (0-24 h or 0-48 h) were prepared by mixing the constant fractions of the different time interval pools. At

selected time points, plasma pools per gender, per time point were prepared by mixing the equal volumes of plasma samples from across the subjects.

Plasma was deproteinized by addition of acetonitrile (1.5 mL of acetonitrile per mL of plasma). The precipitated proteins were removed by centrifugation (10 min at 3000 *g*), and the supernatants were collected and evaporated to dryness. The evaporation residues were redissolved in 1 mL dimethylsulfoxide/water mixture (20/80, v/v). Aliquots (750-850 µL) of redissolved samples were injected on the radio-HPLC system. Similarly fortified predose samples were processed and analyzed along with the test samples. Urine samples were centrifuged and the resultant clear supernatant was injected onto the radio-HPLC system. Aliquots of the methanolic extracts of feces samples were evaporated under nitrogen, and the residues were reconstituted in dimethylsulfoxide/water (1:1, v/v). Aliquots of these samples were injected onto the radio-HPLC system.

Chromatography and spectroscopic studies

HPLC analyses. The HPLC apparatus consisted of a Waters Alliance 2695 gradient pump (Waters, Milford, MA), equipped with automatic injector (Waters Alliance 2695) and a stainless steel Kromasil C_{18} column (30-cm x 4.6-mm i.d., 5 µm, Akzo Nobel). A gradient system with linear steps was applied to the column. Elution started at 1.0 mL/min, with a gradient from 100% of an aqueous solution of 0.05 M ammonium acetate, pH 7.5 (solvent system A), to 45% of solvent system A and 55% of solvent system B over 40 min. Solvent B was composed of an aqueous solution of 0.5 M ammonium acetate, adjusted to pH 7.5/methanol (20:80) (solvent system B). This mobile phase composition was held for 5 min. Subsequently, a linear gradient over 1 min to 100% of solvent system B was applied, and this solvent composition was held for another 5 min before returning to the starting conditions. The column elutes were monitored by

UV-detection set at 218 nm using a Waters 996-diode array detector. On-line radioactivity detection of HPLC-elutes was carried out with a Berthold Radioactivity Monitor LB-509 (Bundoora, Australia). The elutes were mixed with Ultimo Flo^{TM} AP (Packard) as a scintillation cocktail delivered by a Berthold LB-5035-3 pump at a flow rate of 4.0 mL/min. Detector output was connected to the Millennium (Waters) chromatography data system.

The concentration of RWJ-333369 and its metabolites in plasma and urine samples and in fecal extracts were calculated based on the recovery of the radioactivity in the samples and on the areas of the radioactivity peaks obtained after reversed-phase radio-HPLC of appropriate aliquots of these samples. Areas of the radioactivity peaks were converted into disintegrations per minute (dpm) by the data system, after introduction of a calibration curve prepared by injection of known amounts of ^{14}C-RWJ-333369 and a linear regression analysis of the corresponding areas of the radioactivity peaks. The quantitation limit was calculated from the quantitation limit of ^{14}C-RWJ-333369 (200 dpm) and from the amount of radioactivity injected. Samples with known amounts of ^{14}C-RWJ-333369 were injected regularly as controls of the validity of the calibration curve over the whole series of analyses.

Metabolite identification. The metabolites in plasma, urine, and methanolic fecal extracts were identified by HPLC cochromatography with synthetic reference compounds, enzymatic hydrolysis, and/or LC-MS/MS analysis and/or LC-NMR (nuclear magnetic resonance) spectroscopy. For the identification of metabolites by HPLC cochromatography, a mixture of synthetic reference standards (see Fig. 2.) was coinjected with the plasma samples, urine samples, and the methanolic fecal extracts. The synthetic reference standards were monitored by UV-detection (218 nm) (see Fig. 3.), while the radioactive metabolites were monitored by liquid scintillation spectrometry.

For the identification of glucuronide and sulfate conjugates of RWJ-333369 and/or its metabolites in plasma and urine, a comparison was made between the radio-HPLC chromatograms of samples before and after enzymatic hydrolysis with β-glucuronidase/arylsulfatase from *Helix pomatia* (Boehringer Ingelheim GmbH, Ingelheim, Germany; 10 μL/mL acetate-buffered sample, pH 5.0), β-glucuronidase from *Escherichia coli* (Boehringer Ingelheim GmbH, Ingelheim, Germany; 10 μL/mL phosphate-buffered sample, pH 7.0), or arylsulfatase from *Aerobacter aerogenes* (Sigma-aldrich, St. Louis, MO; 10 μL/mL phosphate-buffered sample, pH 7.0). The incubations were performed at 37^{o}C for 24 h.

Representative urine and plasma samples were analyzed by LC-MS/MS (LCQ; Thermo Finnigan MAT, CA, USA, and/or QTof-Ultima Micromass, UK), using a Waters Alliance 2695, a Waters Alliance 2795 or a Surveyor (Thermoquest) separation module with a Waters 996 photodiode-array detector (PDA) or a Surveyor (Thermoquest) PDA detector to confirm the identity of the metabolites and a radioactive monitor (Berthold). A gradient system with linear steps was applied to the column and the chromatographic conditions were identical to those in radio-HPLC analyses. A post column splitter was used to introduce 20 % of the HPLC effluent to the electrospray ionization (ESI) source and 80 % to the waste. LCQ used with ESI and/or atomospheric pressure chemical ionization (APCI) operated in the positive and negative ion modes. The settings (lens voltages, quadrupole and octapole voltage offsets, etc.) of the mass spectrometer were optimized for maximum intensity for RWJ-333369 by using the auto-tune function within the LCQ tune program. Acquired data was processed using Xcaliber^{TM} (version 1.2).

The hybrid quadrupole time-of-flight mass spectrometry (QTof) was used with a dual electrospray ionization probe and was operated in the positive and negative ion mode at a

resolution of 8000 (FWHM at m/z 409.9418 (lock reference)). The source temperature was 100^{o}C, desolvation temperature was 250^{o}C, and the cone voltage was set at 40V. The second LockSpray^{TM} ESI probe provided an independent source of the Lock mass calibrant H_3PO_4 ($M+H^+$) ion at m/z 196.9616 was used as the calibrant. Data acquired in the centroid mode with a scan time of 1 sec and finally processed using Masslynx 4.0 software.

To facilitate the identification of metabolites, several aliquots of urine samples from rat, rabbit and dog studies were concentrated and the metabolites (M8 and M9 from rat, M21, M23 and M24 from rabbit; M11 from dog) were isolated and purified by chromatographic technique. For the confirmation of stereochemistry and position of conjugation, purified conjugated metabolites (M21 and M23) were subjected to enzymatic hydrolysis, followed by chiral analysis, and LC-MS/MS. Chromatographic separation of stereoisomers was achieved by isocratic elution of extracts using a mobile phase (0.02 M ammonium acetate in ethanol/hexane, 20/80) on a chiral column (Chiralpak AD, 5 cm x 4.6 mm I.D.) maintained at ambient temperature. Column elutes were monitored by API 3000 triple quadruple mass spectrometer operated with a turboionspray interface under positive ion mode.

Data analysis

The TR excreted in urine and feces was expressed as a percentage of the administered radioactivity. The mass balance of RWJ-333369 and its metabolites was presented as the percentage of the dose radioactivity accounted for by these radiolabeled compounds. Radioactivity levels in plasma were expressed as microgram-equivalents to RWJ-333369 per mililiter. In plasma, the levels of unchanged RWJ-333369 and metabolites were presented as a percentage of the sample radioactivity. Pharmacokinetic parameters of the total radioactivity in plasma were calculated by noncompartmental analysis using WinNonlin$^{®}$ 4.0.1 (Pharsight,

Mountain View, CA, USA), and the following parameters were estimated: maximum plasma concentration (C_{max}) and corresponding peak time (T_{max}), elimination half-life ($t_{1/2}$), and the area under the plasma concentration-time curve (AUC). The elimination half-life ($t_{½}$) was calculated using the log-linear regression of the terminal plasma concentration *versus* time data. Wherever applicable, pharmacokinetic parameters were presented in mean (± standard deviation).

Results

Excretion of radioactivity

Mean percent recovery of TR in urine and feces for different animal species are summarized in Table 1. After oral administration of ^{14}C-RWJ-333369 to male and female mice, male and female rats, female rabbits, and male dogs, radioactivity was predominantly (all species 86.6%-97.8% of the administered dose, except female mice 60%) recovered in urine and to a very minor extent (4.0%-9.8% of the administered dose) in feces. The rate of excretion was rapid in almost all preclinical species, within the first 24 h post dose about >90% of the administered dose was recovered. Overall excretion was nearly complete at 96 h in all-preclinical species.

Pharmacokinetics of total radioactivity

Mean pharmacokinetic parameters of TR in plasma for mice, rats, rabbits, and dogs are summarized in Table 2. Except in rats, peak plasma concentrations of TR were achieved within 1-2 h. The terminal $t_{1/2}$ of radioactivity ranged from 3.7 h to 6.6 h in mice and rats and ~15 h in rabbits. In dogs, large variations were observed in AUC and $t_{1/2}$ values, and the $t_{1/2}$ was in the range of 9.3 to 84.1 h.

Identification of metabolites

Representative pooled urine radio-chromatographic profiles of mouse, rat, rabbit, and dog are shown in Fig. 4. Metabolites were given a numerical code based on the retention time of metabolites detected in all species.

The MS/MS product-ion ESI mass spectrum of RWJ-333369 shows characteristic fragment ions useful for metabolite identification (Fig. 5.). The fragmentation behavior was dominated by cleavages in the side chain. The MS/MS product ion ESI spectra of the unchanged drug (RWJ-333369) (MH^+ 216) and the retention time of the reference compound R264397 (=RWJ-333369) are identical (Table 3). The presence of other marker ions related to sodium (MH^+ 232) and ammonium (MH^+ 238) adducts of RWJ-333369 confirms the identity of RWJ-333369.

The metabolites of RWJ-333369 identified in various preclinical species along with the method of identification are listed in Table 3. Metabolites ***M1, M4, M5, M14, M21, M22, M23*** and ***M25*** were identified with the synthetic reference compounds as 2-chlorophenylglycine (R342141, CPG), 2-chlorobenzoic acid (R300100, CBA), 2-chloromandelic acid (R288222, CMA), N-acetyl CPG (R338228), *O*-glucuronide of RWJ-333369 (R289876), 4-hydroxy RWJ-333369 (R300592), *O*-glucuronide of RWJ-452399 (R382574) and 1-chloro-2-(1,2-dihydroxyethyl)benzene (R288223), respectively (Fig. 2.). HPLC retention time and MS-MS fragmentation patterns of the synthetic reference compounds were identical to the radioactive peaks (Fig. 3. and Fig. 4., Table 3.).

DMD Fast Forward. Published on January 12, 2007 as DOI: 10.1124/dmd.106.012336
This article has not been copyedited and formatted. The final version may differ from this version.

*Identity of **M2**, **M3**, **M7, M15** and **M17***: Identity of these metabolites was not known. M2 was present in rat and dog, M3/M17 were unique to dog, M7 was present in all preclinical species and M15 was present in rat and mouse.

*Identity of **M8** and **M9***: Metabolites M8 and M9 were identified as pre-mercapturic acid (pre-MACs) conjugates of RWJ-333369. The QTof exact mass of M8, M9 and fragment ions are very close to the calculated exact mass of protonated sodium adduct of pre-MACs of RWJ-333369 (Table 4.) and fragment ions. The protonated molecular ion sodium adduct $(M+Na)^+$ of M8 and M9 was observed at m/z 417.0501 and 417.0476, respectively and the fragmentation patterns were same for M8 and M9. The major fragment ions were m/z 359.0481 (due to loss of sodium and two water molecules), m/z 316.0452 (M8-Na-$2H_2O$-$CONH_2$), and m/z 274.0321 (M8-Na-$2H_2O$-$CONH_2$-$COCH_3$). Based on the fragmentation patterns and NMR analysis (not shown) of the corresponding dehydrated purified metabolites (MAC conjugates of RWJ-333369) from rat urine, M8 and M9 were proposed as pre-MACs of RWJ-333369.

To determine the position of conjugation and hydroxylation on the aromatic ring, attempts were made to synthesize number of possible pre-MACs of RWJ-333369. None of the attempts were successful. However, attempts to synthesize corresponding MACs of RWJ-333369 were successful. About ten aromatic MACs were synthesized and used as reference compounds for the purpose of cochromatographic comparison. The procedure for the synthesis of ten MACs and the HPLC separation data are described in Mannens et al. 2006. Pre-MACs of RWJ-333369 in rat urine were converted to MACs of RWJ-333369 and were cochromatographed with 10 different reference compounds of aromatic MACs of RWJ-333369. Based on these investigations and NMR analysis (data not shown), it was proposed that the N-acetyl-cysteine (NAC) side chains for metabolites M8 and M9 were attached to the aromatic ring at position 5 (meta-position with

respect to aliphatic side chain of RWJ-333369) for metabolite M8 and at position 4 (*para*-position with respect to aliphatic side chain of RWJ-333369) for metabolite M9. The exact position of the hydroxy function and stereochemistry of the metabolites were not determined. Based on the above, the metabolites **M8** and **M9** were identified as pre-MACs of RWJ-333369. In the rat urine, LC-MS/MS analyses revealed that additionally at least three MACs were observed in trace amounts.

*Identity of **M10**, **M11**, **M13**, **M20*** and ***M16***: The ESI mass spectra for metabolites M10, M11, M13, and M20 display the same protonated molecular ion at m/z at 312 (Table 3). A mass shift of 96 compared with RWJ-333369 (protonated molecular ion: 216) points to hydroxylation (16 units), with concomitant sulfate conjugation (80 units). The major fragment ion was observed at m/z 294, arising from the loss of a water molecule directly from the protonated molecular ion indicating the presence of free hydroxyl group in the molecule (see Fig. 6. for protonated mass spectra of M11 in dog urine). Additional fragment ions at m/z 329 and 346 resulting from mono- and di-ammonium adducts of the metabolite were observed in the spectra. Further to mass spectral analysis, radio-HPLC profiles clearly demonstrated that upon enzymatic hydrolysis [with β-glucuronidase/arylsulfatase or arylsulfatase] peaks related to metabolites M11 and M13 disappeared, and there was a concomitant increase in peaks of aglycons (hydroxy RWJ-333369), M16 and M22 (R300592), respectively. These findings and the LC/MS/MS results demonstrate that metabolites **M11** and **M13** are hydroxy-sulfate conjugates of RWJ-333369 and, M16 and M22 (R300592) are monohydroxylated metabolites of RWJ-333369. The position of hydroxylation and sulfate conjugation was determined for metabolite M11 employing ^{1}H NMR and ^{13}C NMR spectroscopy (chemical shifts and coupling constants are not shown) and identity was given as 3-hydroxy sulfate (*ortho* to chloro in the aromatic ring) conjugate of RWJ-333369.

Disappearance of metabolites M10 and M20 in the enzyme-treated samples was not conspicuous; moreover, the percentage of their presence in the urine samples was very low. Based on the LC/MS/MS analysis alone identity was given for metabolites **M10** and **M20** as hydroxy-sulfate conjugates of RWJ-333369.

*Identity of metabolites **M12a,b, M18** and **M19***: Comparison of radio-HPLC chromatograms of enzyme treated [β-glucuronidase or arylsulfatase] *versus* untreated urine samples clearly demonstrated that metabolites M12a,b, M18, and M19 disappeared with a concomitant appearance of corresponding aglycon peaks. Disappearance of these peaks was observed only in samples with β-glucuronidase–treated but not arylsulfatase–treated samples; these findings imply that these metabolites are glucuronide conjugates. Careful examination of radio-HPLC profiles of treated samples indicated that with the disappearance of M12a,b there was a concomitant increase in the peak intensities of metabolites M5 and M4. Based on this finding, it was thought that M12a,b was a mixture of two glucuronides (M12a, M12b), and **M12a,b** was identified as mixture of glucuronides of M4 and M5. Similarly, with the disappearance of M18 and M19 peaks there was a concomitant increase in M25. Hence, **M18** and **M19** are thought to be glucuronides of metabolite M25. Further ESI spectra of M18 and M19 in negative mode showed a deprotonated molecular ion at m/z 347. Marker fragment ions in MS^2 spectra at m/z 175 (glucuronide), 157 (glucuronide – H_2O), and 113 (glucuronide – H_2O –CO_2) were indicative of the presence of a glucuronide in the molecule. Based on molecular and marker fragment ions together with cochromatography of the aglycon (R288223), the identities of **M18** and **M19** were given as glucuronides of M25 [1-chloro-2-(1,2-dihydroxyethyl)benzene].

*Identity of **M24***: In rabbit urine, M24 was extensively studied in both positive and negative modes of ESI iontrap and QTof instruments. The nominal mass of M24 was found to be 295

mass units, but the spectra were dominated by molecular adduct ions (protonated ammonium adduct at m/z 313, protonated 2x ammonium adduct ion at m/z 330) (see Fig. 7.). A mass shift of 80 units from unchanged RWJ-333369 (nominal mass 215) points towards sulfate conjugation. Further fragmentation patterns [at m/z 216, 233 (ammonium adduct of m/z 216), 238 (sodium adduct of m/z 216), 198, 155, 137, 119] are same as that obtained for unchanged RWJ-333369 (Fig. 5.) indicating the direct sulfate conjugation of RWJ-333369. Exact mass data from QTof spectra (in negative mode) (Table 4.) are very close to the calculated exact mass of a deprotonated sulfate conjugate of RWJ333369 points in the same direction as sulfate conjugate of RWJ-333369. From rabbit urine M24 was isolated, purified, and subjected to ^{1}H-NMR spectroscopic analysis. Results indicate (raw data of chemical shifts and coupling constants are not shown) that sulfate conjugation occurred on the aliphatic hydroxy of the side chain of RWJ-333369. Therefore, metabolite **M24** is identified as the sulfate conjugate of RWJ-333369.

Metabolite profile in urine

Urinary metabolites expressed in percent dose radioactivity in different animal species are listed in Table 5. In all preclinical species, radioactivity was predominantly excreted in urine. In rats, after oral administration of ^{14}C-RWJ-333369, less than 2.3% of the dose was excreted unchanged in urine of male and female rats over 0-48 h. Urinary metabolites M1 (2-chlorophenylglycine), M12a,b (mixture of glucuronides of 2-chloromandelic acid and 2-chlorobenzoic acid), M14 (N-acetyl 2-chlorophenylglycine), and M21 (glucuronide of RWJ-333369) were the major metabolites in rats, each ranging from 7.7 to 23.2 % of the administered dose. Other metabolites, M2 (unknown), M4 (2-chlorobenzoic acid), M5 (2-chloromandelic acid), M8 and M9 (pre-MACs of RWJ-333369), M11 and M13 (sulfate conjugates of hydroxy RWJ-333369), M18 and M19 (glucuronide conjugates of M25), M22 (4-hydroxy RWJ-333369), M24 (sulfate conjugate

at the alcohol function of RWJ-333369), and M25 (1-chloro-2-(1,2-dihydroxyethyl) benzene), together contributed to ~29 % of the administered dose within the same period. Metabolites M2, M19, and M25 were specific to rats and were not observed in other species. Metabolite M24 appeared to be specific to female rats and was not detected in male rats.

In mice, less than 2.3 % of the dose was excreted unchanged in male and female mice over 0-24 h (Table 5.). Metabolite M21 was the major metabolite contributing to ~ 44 % of the administered dose in male mice urine within 24 h post dose. M1 and M12a,b were the other predominant metabolites in mice. Pre-MACs of RWJ-333369, M8 and M9, were specific to mice and rats, and were not observed in urinary radio-HPLC profiles of dogs and rabbits.

In rabbits, administered radioactivity was almost completely recovered in urine (Table 5.). Glucuronide (M21, M23) and sulfate (M24) conjugated metabolites were the major metabolites in rabbits and in terms of % dose excreted in urine was 43.6, 15.8 and 31.7 %, respectively. The remainder of the dose was recovered as metabolites M1, M4, M5 (2-chloromandelic acid), M7 (unknown), and M23 (O-glucuronide of R-isomer of RWJ-333369). Metabolites M21 and M23 have been isolated from rabbit urine for NMR-spectroscopy and chiral analysis which clearly showed that the algycon of M21 was RWJ-333369, and the aglycon of M23 was the enantiomer of RWJ-333369 (RWJ-452399). In dogs, metabolites M5, M11, M21, and M23 were the predominant metabolites in urine and in total contributing to about 50% of the administered dose radioactivity within 24 h post dose. Metabolites M3 (unknown), M16 (hydroxy RWJ-333369), and M17 (unknown) were found to be specific to the dog and were not observed in other preclinical species.

Metabolite profile in feces

The percentage of administered radioactivity excreted in feces was very limited in all preclinical species. The extraction recovery of radioactivity from fortified ^{14}C-RWJ-333369 predose fecal samples was in the range of 91.7 % to 98.7 % of the theoretical value. In all animals, the percentage of total radioactivity recovered in the feces was <10% of the administered dose and the majority of the sample radioactivity were contributed by unchanged drug (RWJ-333369). In rats, apart from the unchanged drug, low amounts of metabolites M4, M5, M14, M15, M22, and M25 contributed to sample radioactivity. In dogs, in addition to unchanged drug, low amounts of metabolites M16, M17, M22, and M23 were observed in dog methanolic feces extracts. In mice and rabbits, unchanged drug was by far the predominant peak in the methanolic feces extracts.

Metabolite profile in plasma

The percentages of the plasma sample radioactivity accounted for by the parent drug and various metabolites are listed in Table 6. In the blank plasma samples fortified with ^{14}C-RWJ-333369, the recovery of radioactivity after deproteinization was in the range of 89-131 % of the theoretical value. In all preclinical species, unchanged drug (RWJ-333369) was the predominant component present in plasma. In plasma samples, there was a degradation peak X observed resulting from the carbamoyl migration in RWJ-333369 during sample storage or the sample preparation phase and was confirmed with synthetic reference compound (R307716 structure, see Fig. 2). A similar phenomenon was seen in the predose plasma sample spiked with ^{14}C-RWJ-333369. Hence, parent RWJ-333369 was, in fact, the sum of the radioactive peaks of both RWJ-333369 and its degradation product X (R307716). Carbamoyl migration has been reported in human plasma samples (Mannens et al., 2006).

In the animal species studied, *O*-glucuronide of RWJ-333369 (M21) was the common circulating metabolite present in plasma. In humans, only trace amounts of M21 detected and the levels were below the limit of quantitation of the radio-HPLC method (Mannens et al., 2006). In plasma samples of rats and mice, a mixture of glucuronide conjugates of M4 and M5 (M12a,b) were present, and these were not seen in the dog and rabbit plasma. In contrast to this, M23 (*O*-glucuronide of the R-enantiomer of RWJ-333369) was mainly present in dog and rabbit plasma and was absent in mouse and rat plasma. Among the metabolites in rabbit plasma, sulfate conjugate of RWJ-333369 (M24) was present in significant percentages and was not seen in plasma samples of other animals. In mice, plasma-circulating metabolites were not detected beyond 3 h sample point; it appears that metabolites had shorter plasma half-lives in mice than in other species.

Discussion

The overall metabolism of RWJ-333369 in mice, rats, rabbits, and dogs after single oral administration was evaluated on the basis of the metabolic profiles in urine, feces, and plasma. Given the high recovery of the administered radioactive dose in urine (>85% in almost all species), the overall metabolism was characterized on the basis of urine data. The in vivo metabolic pathway of RWJ-333369 in various preclinical species is presented in Fig. 8.

Similar to humans (Mannens et al., 2006), RWJ-333369 was extensively metabolized in all preclinical species; only minor amounts were excreted unchanged in urine and feces.

Multiple metabolic pathways and renal excretion are involved in the elimination of RWJ-333369 and its metabolites. Some of the major metabolic reaction pathways were glucuronidation, hydrolysis, sulfation, and oxidation.

In mice and rabbits, the *O*-glucuronidation was predominant and most important pathway in the metabolic elimination of RWJ-333369 (Table 5., Fig. 8.). As a primary metabolic step, this pathway was accounted for approximately 24.6 to 44.0 % in mice and 44 % in rabbits. The *O*-glucuronidation of RWJ-333369 (M21) is a single-step reaction (primary metabolic step) due to the presence of the secondary alcohol on the chiral carbon ('S'-enantiomer). *O*-glucuronidation also occurred in combination with chiral inversion at the alcohol function of RWJ-333369 (M23, *O*-glucuronide of 'R'-enantiomer of RWJ-333369). The chiral inversion of RWJ-333369 is a multi-step biotransformation. Although the mechanism of inversion or reversibility of inversion was not elucidated for RWJ-333369, different pathways can be hypothesized as shown for structurally similar chiral alcohols such as stiripentol (Zhang et al., 1994), 1-hydroxyethylpyrene (Landsiedel et al., 1998) and 2-butanol (Krikun and Cedarbaum, 1984). Either redox sequence or sulfate conjugate-mediated inversion mechanisms have been demonstrated for the chiral inversion of alcohol functions. M23 was predominantly present in rabbits than in other species studied. In rats, glucuronidation of secondary metabolites (M4, M5) was more significant than *O*-glucuronidation of UD. Glucuronides of secondary metabolites were not detected in rabbits.

Another distinction among the species was sulfate conjugation (M24), which is a significant metabolic pathway in rabbits but less predominant in other preclinical species (Table 5., Fig. 8.). It appeared that sulfate conjugation, as a primary metabolic step was specific to female animals and absent in male species. With the exception of M24, there were no major gender differences in the metabolism of RWJ-333369 in rodents. Except in rabbits, in all preclinical species examined, there were a number of sulfate conjugates resulting from a secondary metabolic reaction, i.e., aromatic hydroxylation followed by sulfate conjugation (M11, M13).

Metabolites resulting from the hydrolytic, oxidative, and transamination pathways were common to all species (Fig. 8.). In rats and dogs, the combined hydrolytic and oxidative pathways were more predominant than in the other species. Carbamate ester hydrolysis was a key step, which proceeded via multistep biotransformation pathways to different metabolites. Ester hydrolysis is a common metabolic reaction mediated by carboxylesterase(s) and has been observed with many drugs like felbamate (Yang et al., 1991), irinotecan (Humerickhouse et al., 2000), and delapril (Takai et al., 1997). It has been shown that human carboxylesterase isoform-2 mediated the hydrolysis of the carbamate ester in irinotecan. Hydrolysis of the carbamate ester group in RWJ-333369 resulted in the formation of 2-chlorophenylethyl glycol (M25), which was oxidized subsequently to 2-chloromandelic acid (M5) and probably mediated by alcohol and aldehyde dehydrogenases. The α-hydroxy carboxylic acid (2-chloromandelic acid) was converted to 2-chlorobenzoic acid (M4) via oxidative decarboxylation, a metabolic reaction probably common for α-hydroxy acids. Recently, a similar biotransformation has been demonstrated for α-hydroxy bile acid in rat hepatocytes (Merrill et al., 1996). Parallel to the formation of 2-chlorobenzoic acid, 2-chloromandelic acid was biotransformed by transaminases to 2-chlorophenylglycine (M1), most probably via oxidation to 2-chlorophenylglyoxylic acid (an intermediate product).

A similar pathway has been reported for the formation of phenylglycine in the metabolism of styrene (Manini et al. 2002, Haufroid et al. 2002). Styrene was first metabolized to mandelic acid (reference to the formation of 2-chloromandelic acid (M5) in the present study) and subsequently to phenylglycine via phenylglyoxylic acid. Secondary to the above phase-I biotransformations, glucuronide conjugates of 2-chlorophenylethyl glycol (M25), 2-chloromandelicacid (M5) and 2-chlorobenzoicacid (M4) were observed in rodents and dogs, but not in rabbits. In rodents and

dogs, N-acetyl transferases further biotransformed the 2-chlorophenylglycine (M1) to N-acetyl 2-chlorophenylglycine (M14). This conjugative pathway was absent in rabbits. The aromatic hydroxylation of RWJ-333369 was a minor pathway most probably CYP450-mediated, and it was followed by sulphation of the phase-I hydroxy metabolite. This pathway was more predominant in dogs than in any other species.

Two minor metabolites, pre-MACs (pre-mercapturic acid conjugates) of RWJ-333369 (M8, M9), were observed in rodents each accounting for < 2 % and < 3% of the dose in urine of mice and rats, respectively. Identification of metabolites revealed that the N-acetyl-cysteine (NAC) side chains of M8 and M9 were attached to the aromatic ring. These metabolites were most likely formed via arene oxidation, followed by glutathione conjugation, and formation of pre-MACs. The presence of pre-MACs strongly suggests that these metabolites were derived from an arene oxide intermediate, which usually undergoes spontaneous rearrangement to restore aromaticity. However, M8 and M9 appear to be stable pre-MACs of RWJ-333369. Previously stable pre-MACs in urine have been described for bromobenzene (Lertratanangkoon and Horning, 1987). Trace amounts of M8 and M9 were observed in dog urine, and were quantifiable only by LC-MS/MS and not by radio-HPLC analysis (below the limit of quantitation of the radio-HPLC method, <0.3% of the dose). Similar to the dog, in human urine only trace amounts of M8 and M9 were detected by LC-MS/MS analyses (Mannens et al., 2006). Among the four animal species studied, the rabbit was unique in apparently not forming significant extent of metabolites resulting from the oxidative pathways.

Similarities in the metabolic fate of RWJ-333369 in animals and human include *O*-glucuronidation, and hydrolysis of the carbamate ester followed by oxidation to 2-chloromandelic acid and subsequent metabolism to 2-chlorophenylglycine and 2-chlorobenzoic

acid (Mannens et al., 2006). Notable differences were that the N-acetylation pathway and arene-oxidation/glutathione pathway were absent or negligible in humans and non-rodents but present in rodents to a minor extent. All metabolic pathways and metabolites observed in humans were also observed in the preclinical species. Although some glucuronide and sulfate conjugated metabolites were present in plasma, the parent drug was the major plasma circulating drug-related substance in all species studied, including humans.

In summary, the disposition of orally administered RWJ-333369 in animals is characterized by a near complete absorption and extensive metabolism. Consistent with human metabolism, multiple pathways and renal excretion were mainly involved in the elimination of RWJ-333369 and its metabolites in animals.

Acknowledgements

The authors would like to thank Bjorn Verreet (Synthetic Group, Global BA/DMPK, Johnson & Johnson Pharmaceutical Research & Development, Division of Janssen Pharmaceutica N.V., Belgium) and Maurice Hermans (Department of Analytical Development, Johnson & Johnson Pharmaceutical Research & Development, Division of Janssen Pharmaceutica N.V., Belgium) for the synthesis and purification of the metabolite reference compounds, and Dr. Filip Cuyckens (Global BA/DMPK, Johnson & Johnson Pharmaceutical Research & Development, Division of Janssen Pharmaceutica N.V., Belgium) for the critical review of the mass spectral interpretation.

References

Grabenstatter HL and Dudek FE (2004) The use of chronic models in antiepileptic drug discovery: the effect of RWJ-333369 on spontaneous motor seizures in rats with kainate-induced epilepsy. *Epilepsia* **45**(Suppl 7):197.

Haufroid V, Jakubowski M, Janasik B, Ligocka D, Buchet JP, Bergamaschi E, Manini P, Mutti A, Ghittori S, Arand M, Hangen N, Oesch F, Hirvonen A and Lison D (2002) Interest of genotyping and phenotyping of drug-metabolizing enzymes for the interpretation of biological monitoring of exposure to styrene. *Pharmacogenetics* **12**:691–702.

Humerickhouse R, Lohrbach K, Li L, Bosron WF and Dolan ME (2000) Characterization of CPT-11 hydrolysis by human liver carboxylesterase isoforms hCE-1 and hCE-2. *Cancer Res* **60**:1189–1192.

Krikun G and Cederbaum AI (1984) Stereochemical studies on the cytochrome P-450 and hydroxyl radical dependent pathway of 2-butanol oxidation by microsomes from chow-fed, Phenobarbital treated, and ethanol-treated rats. *Biochemistry* **23**:5489–5494.

Landsiedel R, Pabel U, Engst W, Ploschke J, Seidel A and Glatt H. (1998) Chiral inversion of 1-hydroxyehtylpyrene enantiomers mediated by enantioselective sulfotransferases. *Biochem Biophys Res Comm* **247**:181–185.

Lertratanangkoon K and Horning MG (1987) Bromobenzene metabolism in the rat and guinea pig. *Drug Metab Dispos* **15**:1–11.

Manini P, Andreoli R, Poli D, De Palma G, Mutti A and Niessen W (2002) Liquid chromatography/electrospray tandem mass spectrometry characterization of styrene metabolism in man and rat. *Rapid Commun Mass Spectrom* **16**:2239–2248.

Mannens G.S.J, Hendrickx J, Janssen C, Chien S, Van Hoof B, Verhaeghe T, Kao M, Kelley MF, Goris I, Bockx M, Verreet B, Meuldermans W and Bialer M (2006) The absorption, metabolism and excretion of the novel neuromodulator RWJ-333369 in humans. *Drug Metab Dispos* (in Press, Aug 2006).

Merrill JR, Schteingart CD, Hagey LR, Peng Y, Ton-Nu H-T, Frick E, Jirsa M and Hofmann AF (1996) Hepatic biotransformation in rodents and physiochemical properties of 23(R)-hydroxychenodeoxycholic acid, a natural a-hydroxy bile acid. *J Lipid Res* **37**:98–112.

Nehlig A, Rigoulot M, Boehrer A (2005) A new drug RWJ-333369 displays potent antiepileptic properties in genetic models of absence and audiogenic epilepsy. *Epilepsia* **46**(Suppl 8):215.

Takai S, Matsuda A, Usami Y, Adachi T, Sugiyama T, Katagiri Y, Tatematsu M and Hirano K (1997) Hydrolytic profile for ester-or amide linkage by carboxylesterases pl 5.3 and 4.5 from human liver. *Biol Pharm Bull* **20**:869–873.

Yang JT, Adusumalli VE, Wong KK, Kucharczyk N and Sofia RD (1991) Felbamate metabolism in the rat, rabbit, and dog. *Drug Metab Dispos* **19**:1126–1134.

Zhang K, Tang C, Rashed M, Cui D, Tombret F, Botte H, Lepage F, Levy, RH and Baillie TA (1994) Metabolic chiral inversion of stiripentol in the rat I. Mechanistic studies. *Drug Metab Dispos* **22**:544–553.

Figure legends

Fig. 1. Chemical structure of ^{14}C-RWJ-333369 with the position of the ^{14}C-label indicated by with an asterisk (*).

Fig. 2. Chemical structures of the reference compounds cochromatographed with urine, feces, and plasma samples from all species dosed with ^{14}C-RWJ-333369.

Fig. 3. UV-chromatogram obtained for a mixture of reference compounds, which was cochromatographed with urine, feces, and plasma samples from mice, rats, rabbits, and dogs dosed with ^{14}C-RWJ-333369.

Fig. 4. Representative urine sample radio-HPLC chromatographic profiles of mouse (a), rat (b), rabbit (c), and dog (d) following single oral administration of ^{14}C-RWJ-333369 (metabolites are indicated with numbers and RWJ-333369 as UD [unchanged drug]).

Fig. 5. Characteristic mass spectral fragment ions of RWJ-333369 in the positive mode of electrospray ionization mass spectrometry.

Fig. 6. Mass spectral fragmentation pattern of M11.

Fig. 7. Mass spectral fragmentation pattern of M24.

Fig. 8. Metabolic pathways of RWJ-333369 after a single oral dose in the mouse, rat, rabbit, and dog. (The metabolite code is given in parentheses: M, mouse; R, rat; Rb, rabbit; D, dog).

DMD Fast Forward. Published on January 12, 2007 as DOI: 10.1124/dmd.106.012336
This article has not been copyedited and formatted. The final version may differ from this version.

Table 1. Mean (± SD) excretion of total radioactivity in urine and feces of mice, rats, rabbits, and dogs after single oral administration of ^{14}C-RWJ-333369.

Species	Dose (mg/kg)	Radioactive dose (MBq)	No. of animals	Excretion (%) in Urine	Excretion (%) in Feces	Total* excretion
Male mice	50	0.030	12	86.63 ± 7.10	4.01 ± 1.47	98.12 ± 0.83
Female mice	50	0.020	12	60.09± 12.61	8.14 ± 6.00	90.45 ± 6.45†
Male rats	30	0.360	5	89.11 ± 3.79	9.77 ± 3.02	100.28 ± 0.73
Female rats	30	0.310	5	88.95 ± 5.36	9.09 ± 3.15	100.25 ± 2.48
Female rabbits	100 (200)	5.54 (10.52)	2 (1)	97.79 ± 8.13	7.69 ± 2.60	106.11 ± 8.18
Male dogs	20	12.390	4	89.09 ± 3.25	7.37 ± 2.44	98.05 ± 3.45

*Including recovery from cage washings/debris.

†Significant amount recovered in cage washings/debris.

Table 2. Pharmacokinetic parameters of total radioactivity in plasma samples after single oral administration of ^{14}C-RWJ-333369 in mice, rats, rabbits, and dogs.

Parameter	Mice[1] (50 mg/kg)		Rats[1] (30 mg/kg)		Female rabbits		Male dogs[4]
	Male	Female	Male	Female	(100 mg/kg)[2]	(200 mg/kg)[3]	(20 mg/kg)
C_{max} (μg eqv./mL)	25.3	20.2	15.6	15.6	83.4	97.8	24.6 (± 1.75)
T_{max} (h)	1.0	1.0	3.0	3.0	1.5	2.0	1.8 (± 0.50)
$t_{½}$ (h)	3.7	4.1	6.6	5.6	14.6	15.8	44.9 (± 38.0)
AUC_{0-t} (μg eqv.h/mL)	95.8	93.6	174.8	177.5	654.7	1119.9	215.0 (± 246.2)
AUC_{0-inf} (μg eqv.h/mL)	97.3	95.6	192.0	188.0	663.2	1133.6	222.1 (± 285.4)

[1]Data derived from pooled plasma; [2]mean of two animals; [3]data from one animal; [4] mean (± S.D) from four animals. C_{max} = maximum plasma concentration; T_{max},= corresponding peak time; $t_{1/2}$ = elimination half-life; AUC =area under the plasma concentration-time curve.

Table 3. Identity of various metabolites of RWJ-333369 in mice (M), rats (R), rabbits (Rb), and dogs (D) after single oral administration of ^{14}C-RWJ-333369.

Met #	Species	Identification method	Identity	MH^+ or M^- or MA	Typical MS or MS^2 or 3 fragments
UD	M, R, Rb, D	Co-chromatography, LC-MS/MS	RWJ-333369, unchanged drug (UD)	216, 232, 238	119, 137, 155, 198
M1*	M, R, Rb, D	Co-chromatography, LC-MS/MS	R342141, 2-chlorophenylglycine (CPG)	186	140, 169
M4*	M, R, Rb	Co-chromatography, LC-MS/MS	R300100, 2-chlorobenzoic acid (CBA)	155	111
M5*	M, R, Rb, D	Co-chromatography, LC-MS/MS	R288222, 2-chloromandelic acid CMA)	185	141, 123, 111
M8	M, R	LC-MS/MS, NMR	Pre-MAC of UD	417, 395	274, 298, 316, 359, 377
M9	M, R	LC-MS/MS, NMR	Pre-MAC of UD	417, 395	274, 316, 359, 377

M10	D	LC-MS/MS	Sulfate conjugate of hydroxyl-UD	312, 329, 346	294
M11	M, R, D	LC-MS/MS, NMR	Sulfate conjugate of 3-hydroxy -UD	312, 329, 346	294
M12a,b*	M, R, D	Hydrolysis	A mixture of glucuronides of CMA and CBA	-	-
M13	M, R, D	LC-MS/MS	Sulfate conjugate of hydroxy UD	312, 329, 346;	294
M14*	M, R, D	Co-chromatography, LC-MS/MS	R338228, N-acetyl derivative of CPG	228	140, 169, 182, 186, 210
M16	D	Hydrolysis, LC-MS/MS of M11	3-hydroxy UD	-	-
M18	R, D	Hydrolysis, LC-MS/MS	Glucuronide of M25	347	84, 85, 113, 157, 175, 210
M19	R	Hydrolysis, LC-MS/MS	Glucuronide of M25	347	84, 85, 113, 157,

					175, 210
M20	M, D	LC-MS/MS	Sulfate conjugate of hydroxyl UD	312, 329, 346	294
M21*	M, R, Rb, D	Co-chromatography, Hydrolysis, LC-MS/MS	R289876, Glucuronide of UD	409	198, 216, 374, 392
M22*	M, R	Co-chromatography, LC-MS/MS	R300592, 4-hydroxy UD	230	211, 169, 230
M23*	M, Rb, D	LC-MS/MS, NMR, chiral analysis, co-chromatography	O-glucuronide of RWJ-452399 (the other enantiomer of UD)	409, 392	198, 216, 374, 392
M24	M, R, Rb	LC-MS/MS, NMR	Sulfate conjugate at the alcohol function of UD and/or of its enantiomer	330, 313, 295	119, 137, 155, 198, 238, 233, 216
M25*	R	Co-chromatography	R288223, 1-chloro-2-(1,2-dihydroxyethyl) benzene	-	-

Identity of M2 (rat), M3 (dog), M7 (mouse, rat, dog and rabbit), M15 (mouse, rat), M17 (dog) is unknown. MA: molecular adduct of NH_3^+ or Na^+; LC-MS/MS = liquid chromatography-tandem mass spectrometry; NMR = nuclear magnetic resonance; pre-MAC = premercapturic acid conjugate. (*)Identified with synthetic reference standard

Table 4. QTof exact mass data of metabolites M8, M9, M21, M23, and M24

Metabolite	Operation Mode	Exact Mass	mDa	Ppm	Calculated Mass	Formula, Proposed identity
M8	Positive	417.0501	0.2	0.4	417.0499	C14H19N2O7SCl Na, Pre-MAC of RWJ-333369
M9	Positive	417.0476	-2.8	-5.5	417.0499	C14H19N2O7SCl Na, Pre-MAC of RWJ-333369
M21 (R289876)*	Positive	392.0741	-0.8	2.0	392.0748	C15H19NO9Cl, Glucuronide conjugate of RWJ-333369
M23 (R382574)*	Positive	392.0757	0.9	2.2	392.0748	C15H19NO9Cl, Glucuronide conjugate of RWJ-452399
M24	Negative	293.9855	16	5.4	293.9839	C9H9NO6SCl, Sulfate conjugate of RWJ-333369

* Synthetic reference standard for the metabolite

Table 5. Mass balance of unchanged RWJ-333369 (UD) and its metabolites in urine of mice, rats, rabbits, and dogs after single oral administration of ^{14}C-RWJ-333369. (-) Represents not detected and/or below the quantitation limit (200 dpm).

	Mice (50 mg/kg)*		**Rats (30 mg/kg)***		**F. rabbits***	**Male dogs***
Metabolite	**(0-24 h)**		**(0-48 h)**		**(0-48 h)**	**(0-24 h)**
	Male	**Female**	**Male**	**Female**	**100 mg/kg**	**20 mg/kg**
RWJ-333369	0.8	1.4	1.6	2.3	0.3	0.5
M1	13.5	5.9	7.7	12.3	3.4	5.3
M2	-	-	0.3	1.2	-	0.4
M3	-	-	-	-	-	6.8
M4	1.2	2.7	6.4	5.8	6.1	-
M5	6.8	4.9	3.4	2.6	2.3	8.6
M7	-	-	0.3	1.1	3.0	2.5
M8	0.6	0.4	2.0	2.6	-	-
M9	1.3	1.5	2.8	2.3	-	-
M10	-	-	-	-	-	2.0
M11	2.0	1.1	3.4	2.1	-	18.4
M12a,b	7.9	5.9	23.2	18.7	-	1.9
M13	2.1	1.3	1.7	0.6	-	2.1

M14	1.9	1.4	12.7	9.2	-	1.5
M15	2.0	1.8	-	-	-	-
M16	-	-	-	-	-	0.6
M17	-	-	-	-	-	1.5
M18	-	-	2.1	1.6	-	1.2
M19	-	-	1.5	1.5	-	-
M20	0.8	0.9	-	-	-	4.9
M21	44.0	24.6	8.0	9.4	43.6	14.7
M22	1.1	0.8	1.2	1.7	-	-
M23	2.3	1.9	-	-	15.8	8.1
M24	-	5.0	-	3.8	31.7	-
M25	-	-	0.7	0.0	-	-
Total	88.3	61.5	78.6	78.9	106.2	80.9

*Figures represent the percentage of the dose radioactivity. UD = unchanged drug; dpm = disintegrations per minute.

Table 6. Relative amounts of RWJ-333369 (UD) and its major metabolites in the overall pools of plasma samples from animal species following single oral administration of ^{14}C-RWJ-333369. Figures represent the percentage of the sample radioactivity. (-) represents analyte below the quantitation limit (200 dpm).

Time (h)	UD*	M21	M12a,b	M23	M24
Male mice (50 mg/kg)					
1 h	66.4	19.5	3.0	-	-
3 h	30.0	25.3	7.4	-	-
8 h	53.1	-	-	-	-
24 h	-	-	-	-	-
Female mice (50 mg/kg)					
1 h	62.7	8.9	4.0	-	-
3 h	24.9	10.3	5.3	-	-
8 h	25.2	-	-	-	-
24 h	-	-	-	-	-
Male rats (30 mg/kg)					
1 h	89.1	1.6	3.3	-	-
3 h	83.6	1.0	2.9	-	-

8 h	93.2	1.5	6.2	-	-
24 h	49.3	<2.9	17.6	-	-
Female rats (30 mg/kg)					
1 h	98.3	1.6	3.0	-	-
3 h	81.9	2.1	3.9	-	-
8 h	79.3	1.9	8.4	-	-
24 h	98.3	1.6	3.0	-	-
Male dogs (20 mg/kg)					
1 h	76.1	4.9	-	1.6	-
4 h	63.1	7.9	-	5.1	-
8 h	46.4	7.5	-	6.4	-
24 h	18.4	4.5	-	3.4	-
Female rabbits (100 mg/kg)					
1 h	68.8	7.5	-	2.6	18.3
4 h	51.1	7.9	-	4.8	20.0
8 h	36.8	11.2	-	8.3	12.9
24 h	Not done	Not done	Not done	Not done	Not done

*Includes compound X resulting from carbomyl migration during the storage of plasma, as confirmed from the spiked control plasma samples. dpm = disintegrations per minute.

DMD Fast Forward. Published on January 12, 2007 as DOI: 10.1124/dmd.106.012336
This article has not been copyedited and formatted. The final version may differ from this version.

Fig. 1.

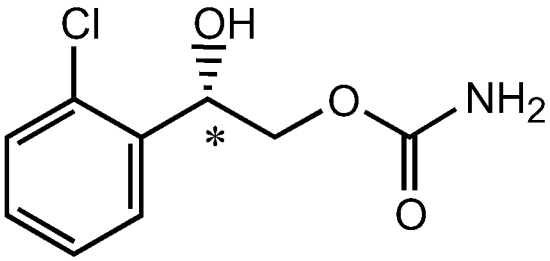

DMD Fast Forward. Published on January 12, 2007 as DOI: 10.1124/dmd.106.012336
This article has not been copyedited and formatted. The final version may differ from this version.

Fig. 2.

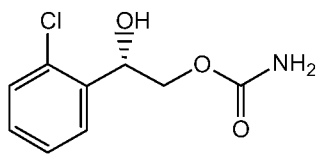

RWJ-333369 = UD

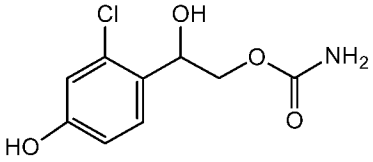

R300592 = M22

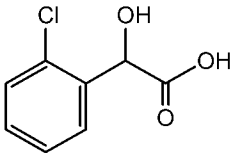

R288222 = M5

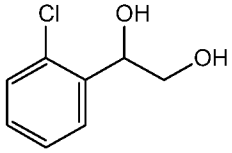

R288223 = M25

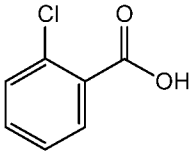

R300100 = M4

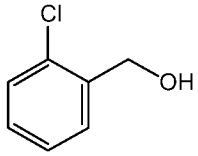

R300099

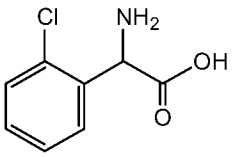

R342141 = M1

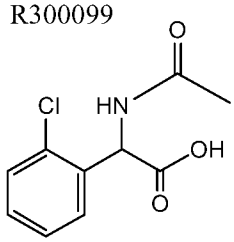

R338228 = M4

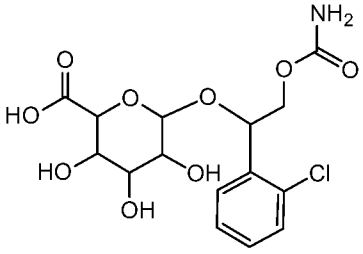

R289876 = M21

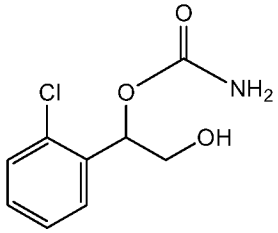

R307716 = X

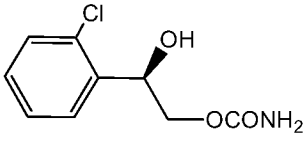

RWJ-452399
(Aglycone of M23)

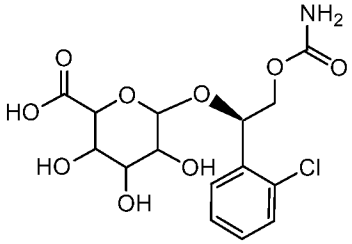

R382574 = M23

DMD Fast Forward. Published on January 12, 2007 as DOI: 10.1124/dmd.106.012336
This article has not been copyedited and formatted. The final version may differ from this version.

Fig. 3.

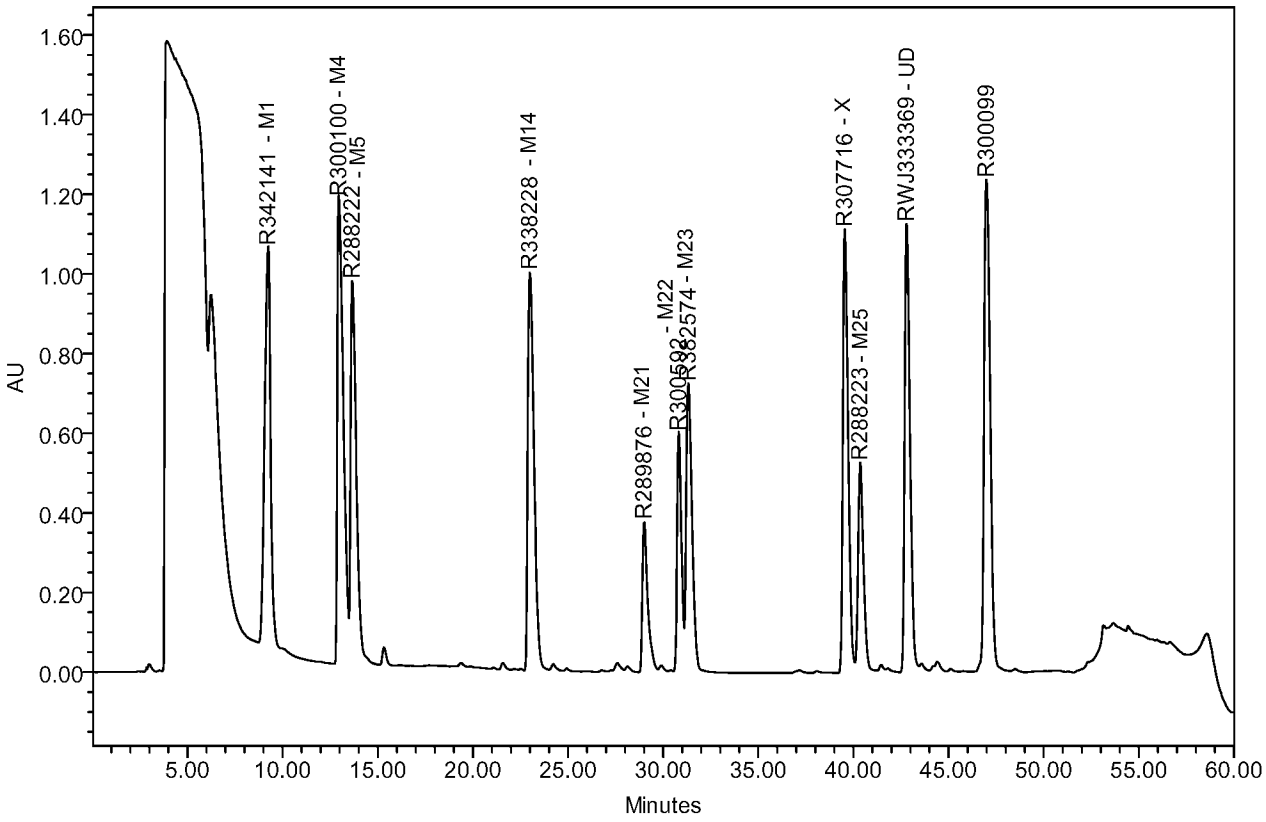

DMD Fast Forward. Published on January 12, 2007 as DOI: 10.1124/dmd.106.012336
This article has not been copyedited and formatted. The final version may differ from this version.

Fig. 4.

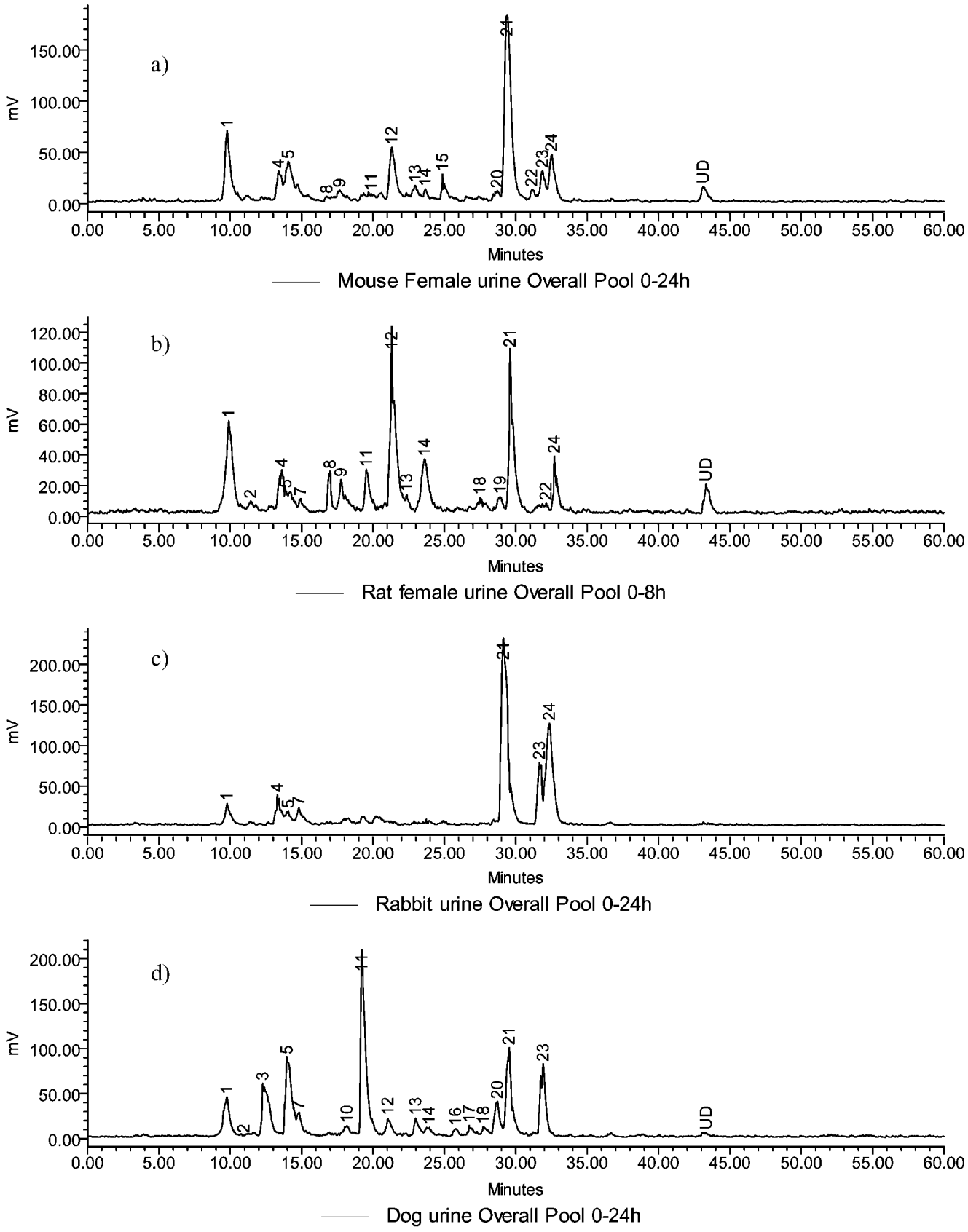

DMD Fast Forward. Published on January 12, 2007 as DOI: 10.1124/dmd.106.012336
This article has not been copyedited and formatted. The final version may differ from this version.

Fig. 5.

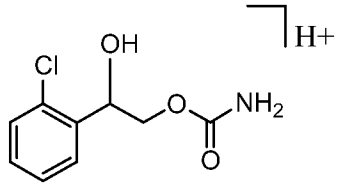

$C_9H_{11}ClNO_3^+$

Exact Mass: 216.0427

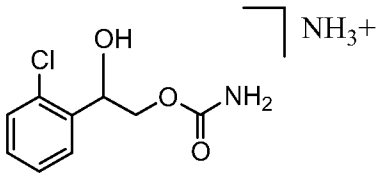

$C_9H_{13}ClN_2O_3$

Exact Mass: 232.0615

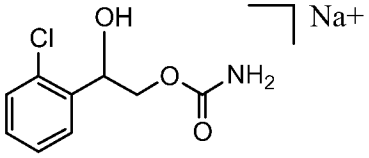

$C_9H_{10}ClNNaO_3$

Exact Mass: 238.0247

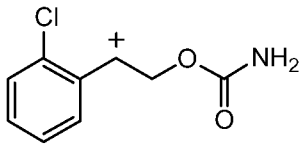

$C_9H_9ClNO_2^+$

Exact Mass: 198.0322

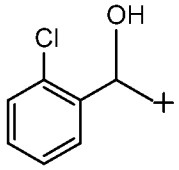

$C_8H_8ClO^+$

Exact Mass: 155.0264

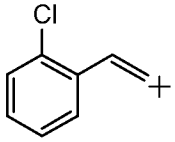

$C_8H_6Cl^+$

Exact Mass: 137.0158

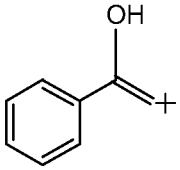

$C_8H_7O^+$

Exact Mass: 119.0497

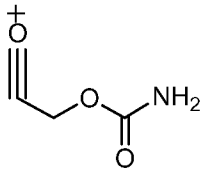

$C_3H_4NO_3^+$

Exact Mass: 102.0191

Fig. 6.

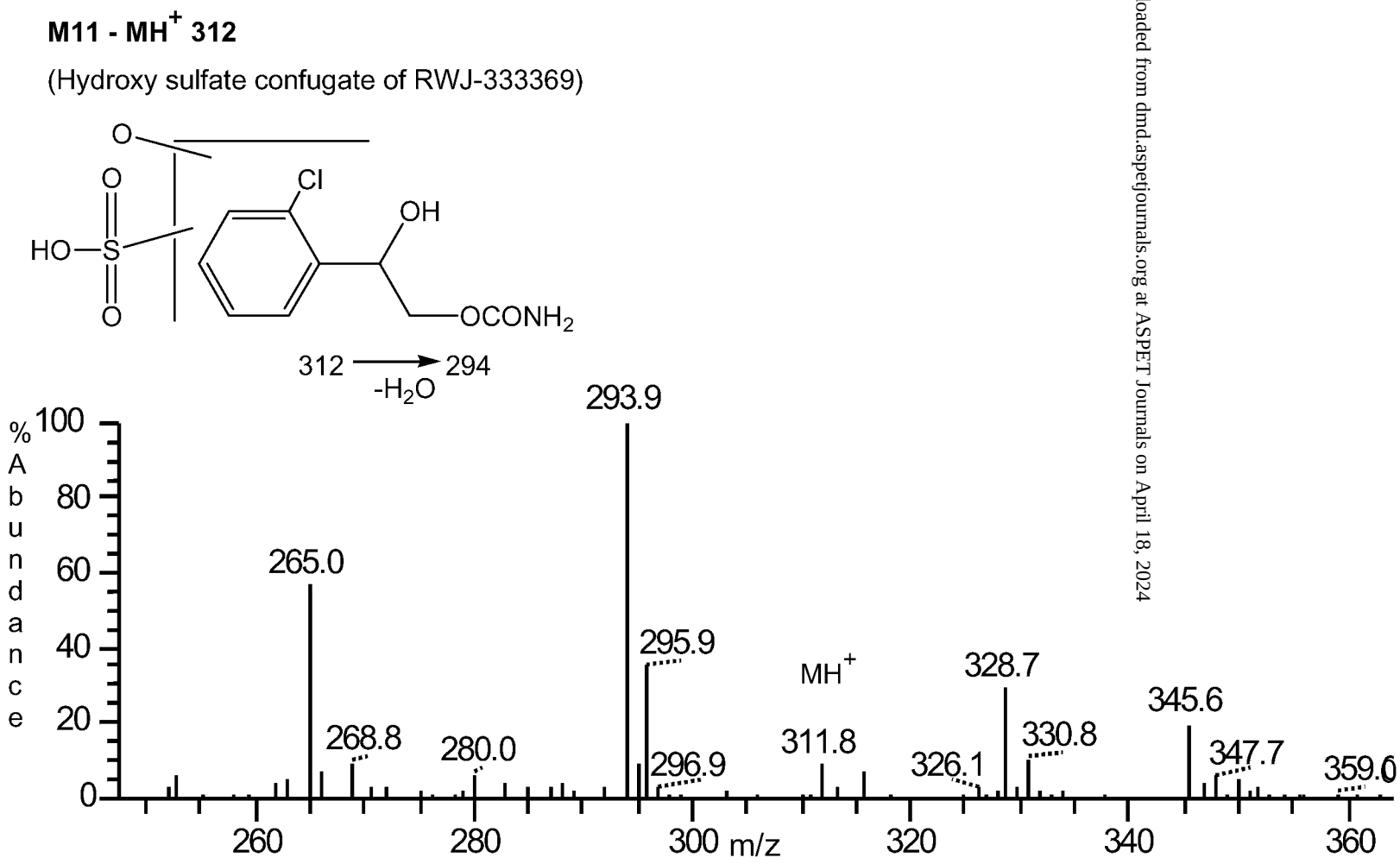

Fig. 7.

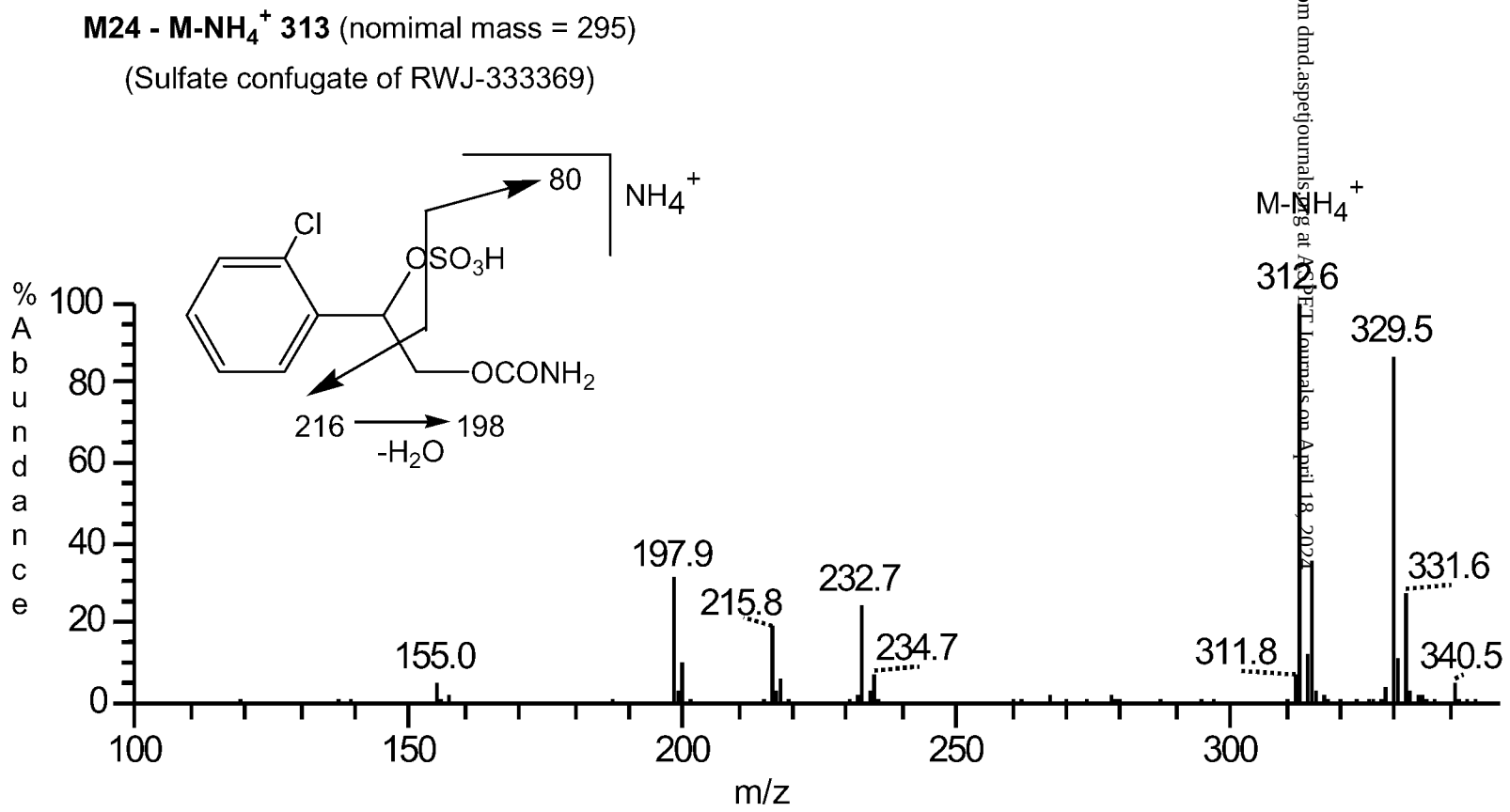

Fig.8.